Electronic Supplementary Material (ESI) for New Journal of Chemistry.
This journal is © The Royal Society of Chemistry and the Centre National de la Recherche Scientifique 2019

## Supporting Information

# Distinctively complete inhibition of fibrillation of serum albumins by methotrexate in vitro: Experimental and modelling studies to understand the tuning of protein misfolding-related aggregations

**Deb Kumar Khatua and Mintu Halder***

Department of Chemistry

Indian Institute of Technology, Kharagpur-721302, India

E-mail: mintu@chem.iitkgp.ac.in

## 1. EXPERIMENTAL SECTION

### 1.1. Materials

BSA (Sigma ID A7030, fatty acid and globulin free), HSA (Sigma ID A3782, fatty acid and globulin free), Folic acid, Methotrexate, Thioflavin T were purchased from Sigma-Aldrich. Other chemicals are of analytical reagent grade. All other experiments were carried out in 20 mM phosphate buffer solution of pH 7.4. Ultrapure water was used for all solution preparations. The pH of buffer solutions was measured with a pre-calibrated EUTECH pH 510 ion pH-meter.

### 1.2.Methods

#### 1.2.1. Induction of aggregation

SAs (10 μM) were incubated at 65 °C for a definite time period to induce their fibrillation and the effect of Folic acid and Methotrexate on thermally-induced aggregation of the said proteins was studied by different experiments.

#### 1.2.2. Tryptophan fluorescence

All steady-state fluorescence emission measurements were taken on a JobinYvon-Spex Fluorolog-3 spectrofluorimeter, using a 0.4 cm path length quartz cuvette. BSA concentration was kept at $1\times10^{-5}$ M for all the fluorescence measurements. Excitation of BSA was done at 295 nm. Emission spectra were collected from 310 to 500 nm, keeping the excitation slit at 2 nm and emission slit at 1 nm.

#### 1.2.3. CD study

CD spectra were recorded on a JASCO-810 automatic recording spectropolarimeter at 298 K over a wavelength range of 190−260 nm with a scan speed 50 nm/min under constant nitrogen flushing. A quartz cell having path length 0.1 cm was used, and two successive scans were accumulated for each spectrum. The baseline was corrected with buffer solution running under the same condition as blank and subtracted from the experimental spectra. The concentration of BSA was taken as 4 μM. The data were fitted with DichroWeb software.[1, 2]

### 1.2.4. Thioflavin T fluorescence study

Thioflavin T (ThT) fluorescence was recorded by excitation at 450 nm in the presence of BSA. Concentrations of both BSA and ThT used were $1 \times 10^{-5}$ M. Emission spectra were collected from 465 to 650 nm, keeping the excitation slit at 3 nm and emission slit at 2 nm. The kinetic traces of the evolution of ThT fluorescence intensity[3, 4] was fitted to the following multiexponential equation: $F = F_\infty + \Delta F(-kt)^n$, where '$F$' is the observed fluorescence intensity at any time '$t$', '$F_\infty$' is the final intensity, '$\Delta F$' is the difference between the initial and final intensities, '$k$' is the rate constant of aggregation, and '$n$' is a number signifying the cooperativity of aggregation.

### 1.2.5. Scanning Electron Microscopy (SEM)

The morphology of protein aggregates was examined on a field emission scanning electron microscopy (FESEM) (Carl Zeiss MERLIN) using aluminum foil with an acceleration voltage of 5 keV.

### 1.2.6. Native Gel-electrophoresis

Native gel electrophoresis was performed in Bio-Rad mini protean tetra cell electrophoresis system by using 12% polyacrylamide gel with a constant voltage of 80 V. 10 μL samples were loaded in each well keeping protein concentration at 10 μM.

### 1.2.7. Docking and AGGRESCAN study

For docking experiments, we have used SYBYL X 2.1 and Discovery Studio Visualizer 4 from Accelrys Software Inc., and for aggregation-propensity calculation we have used AGGRESCAN tool.[5] The crystal structures of BSA (PDB ID: 4F5S)[6] and HSA (PDB ID: 1AO6)[7] from protein data bank were used for docking and AGGRESCAN studies. For optimization of FA and MTX structure Tripos force field and Gasteiger-Hückel charges were used considering gradient convergence criteria 0.01 kcal/mol. For Surflex-Docking experiment, first protein structure was analyzed and essential hydrogen atoms and charges were

added. Protomol was created keeping threshold and bloat parameters 0.2 and 1, respectively. Other parameters were kept at their default values. We have taken 200 output poses in this study and considered top 20 poses according to the Total-score for data analysis.

### 1.2.8. Molecular dynamics simulation study

The dynamic behavior for BSA and BSA-docked complex were followed by molecular dynamics (MD) simulations by using GROMACS 5.1.4.[8, 9]The topology parameters for FA and MTX molecules were generated by the LigParGen online server.[10]All calculations were performed using GROMACS inbuilt analysis tools. Periodic boundary conditions were applied with OPLS force fields during all simulations.[11] The BSA and BSA-docked complex were subjected to solvated simple point charge (SPC) method with 34217, 34221 and 34221 water molecules. Further, these water molecules were surrounded within the box with diameter 12.0, 9.0, 10.5 nm, where the protein was kept at the center of the box for all systems. Further, 16 $Na^+$ ions were added to neutralize the charge of systems. All systems were energy minimized using the steepest descent method. Further the whole system was equilibrated for 1 ns in NVT ensemble (constant Number of molecules, Volume, and Temperature) using modified Berendsen thermostat coupling with coupling constant of 0.1 ps followed by 1 ns NPT ensemble (constant Number of molecules, Pressure, and Temperature) using Berendsen barostat to obtain stable pressure of 1 bar. Lastly, 100 ns MD simulations were performed for all systems at two different temperatures with 2 fs time step using Parrinello–Rahman pressure coupling.[12, 13]

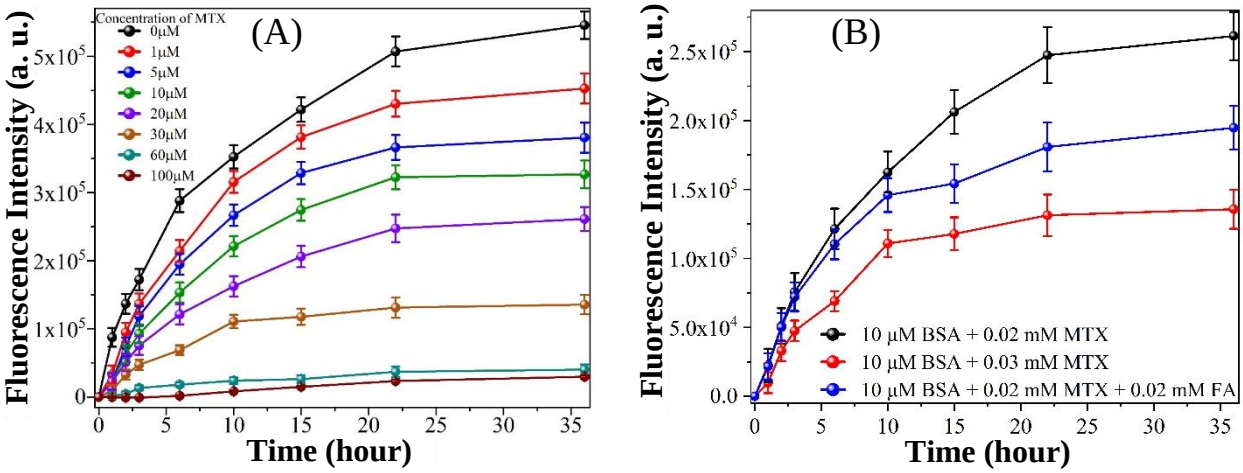


**Fig. S1.** Kinetics of BSA (10 μM) fibrillation by monitoring ThT (10 μM) fluorescence as a function of MTX concentration (A), and MTX/ MTX+FA concentration (B). ThT fluorescence was recorded at 484 nm with 450 nm excitation (symbol with cap indicates error bar).

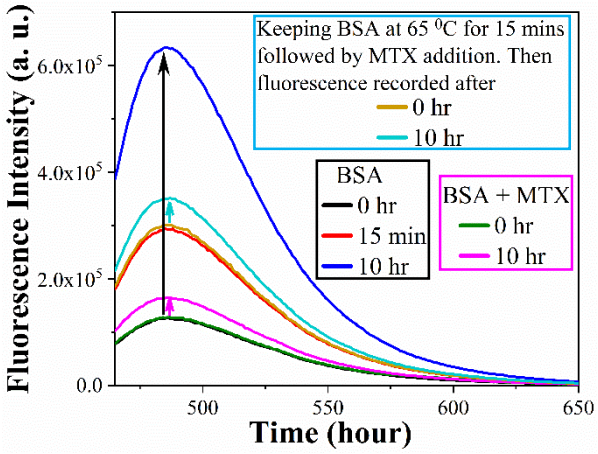


**Fig. S2.** BSA (20 μM) fibrillation studied without MTX (black lines), with MTX (0.1 mM, red and blue lines) by monitoring ThT (10 μM) fluorescence with 450 nm excitation. After 15 minutes of incubation of BSA at 65 $^0$C, MTX was added and fibrillation was monitored after 10 hours (blue lines). In all cases the final mixtures were incubated at 65 $^0$C for 10 hours.

Here, we observed that the presence of MTX, even at this stage, substantially prevented further rise in ThT fluorescence. This perhaps clearly indicates that the presence of MTX at any stage drastically inhibits fibrillation. It could possibly be due to the interaction of unreacted (may be monomeric) population of BSA. That is why we observed almost complete arresting of fibrillation of BSA when MTX was added at the very beginning of the process. It may be noted that the study further indicates that if MTX is present at the start of the process, the inhibition goes to the fullest extent. So, it may be quite possible that the binding of MTX with BSA can have a very significant role in the inhibition of BSA fibrillation.

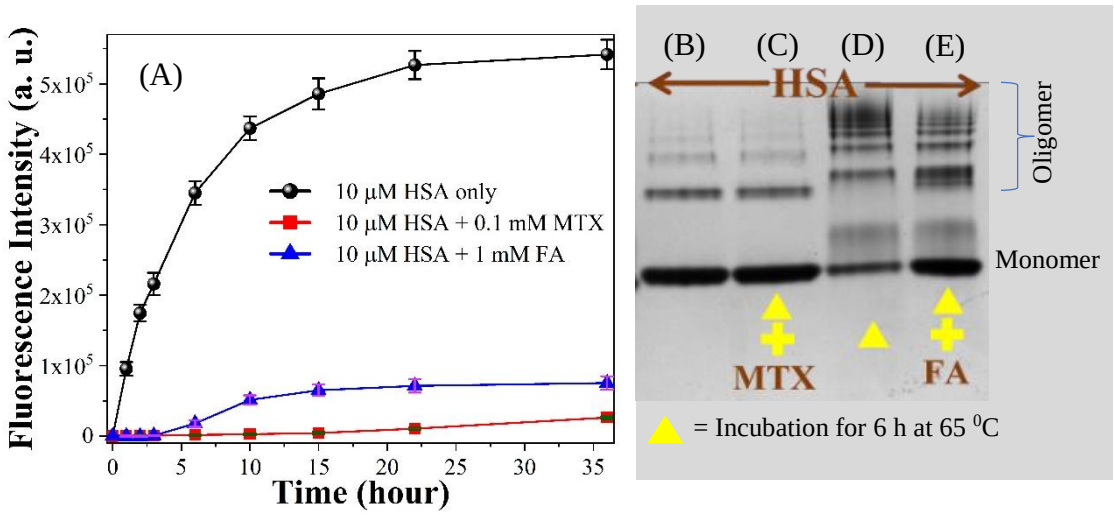


**Fig. S3.** Kinetics of HSA fibrillation (A) studied by monitoring ThT (10 μM) fluorescence in presence of 0.1 mM MTX and 1 mM FA. ThT fluorescence was recorded at 484 nm with 450 nm excitation. Native gel electrophoresis of (B) HSA without heating, (C) HSA in 0.1mM MTX, (D) HSA, (E) HSA in 1 mM FA, after incubation of 6 hours at 65 $^0$C for all the cases, except with B.

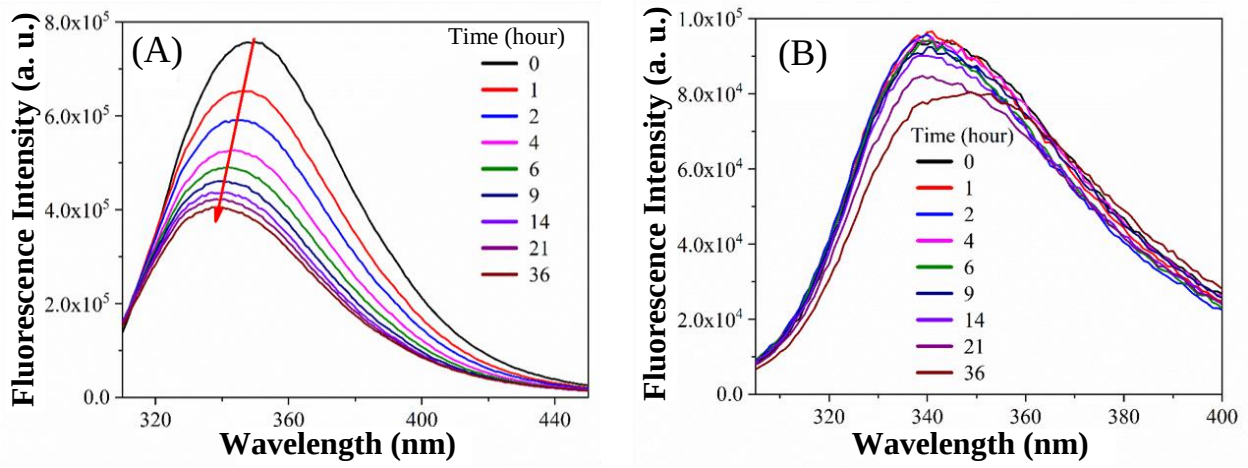


**Fig. S4.** Tryptophan fluorescence emission spectra of BSA (10 μM) at different incubation time at 65 $^0$C without MTX (A) and with MTX (B), respectively. BSA was excited at 295 nm.

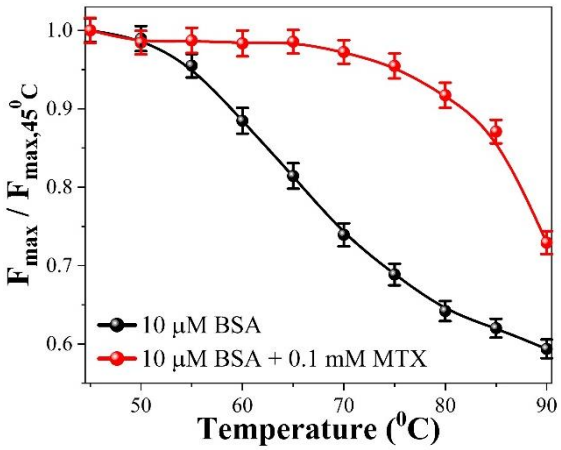


**Fig. S5.** Thermal stability of BSA and BSA-MTX complex. The solutions were incubated at different temperatures for 15 minutes. Excitation of BSA was made at 295 nm. Emission spectra were collected from 310 to 450 nm. Protein unfolding was measured by the change in maximum fluorescence intensity (ratio of maximum fluorescence intensity at different temperatures and maximum fluorescence intensity at 45 $^0$C). Concentration of BSA and MTX were 10μM and 0.1 mM, respectively.

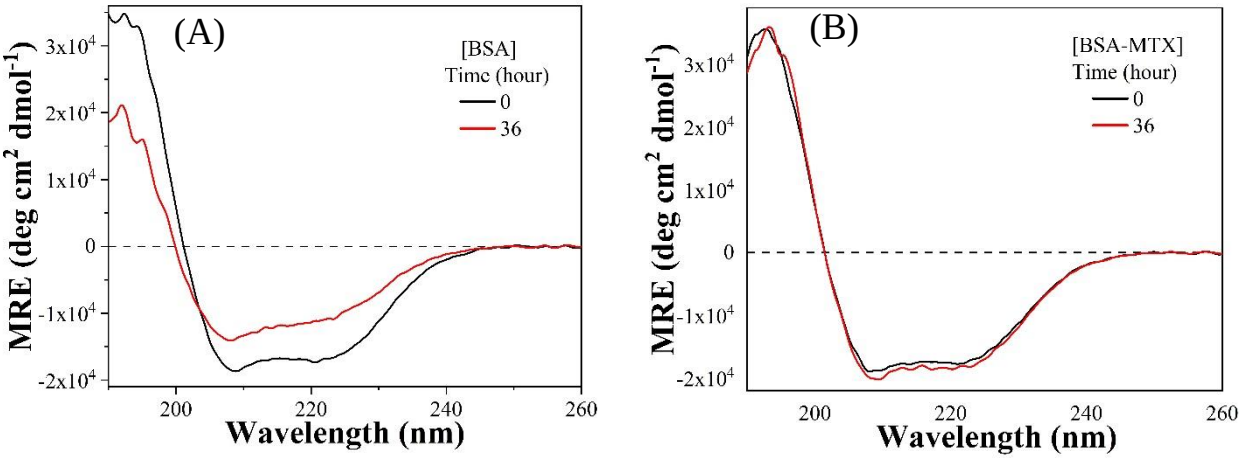


**Fig. S6.** CD spectra of BSA (4 μM) without MTX (A) and with MTX (B), respectively.

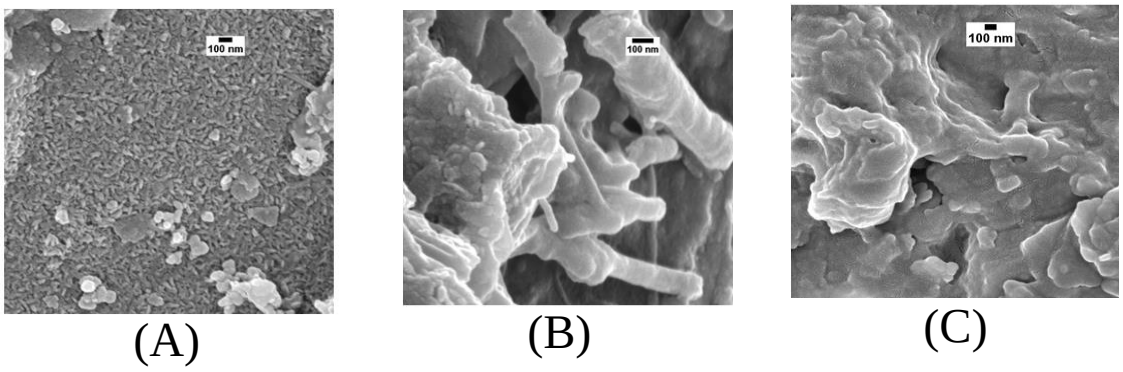


**Fig. S7.** SEM images of (A) HSA fibril, (B) HSA incubated with Folic Acid, (C) HSA incubated with Methotrexate. The samples were incubated in 20mM phosphate buffer and 100 mM NaCl at pH 7.4 at 65 $^{0}$C for 5 days.

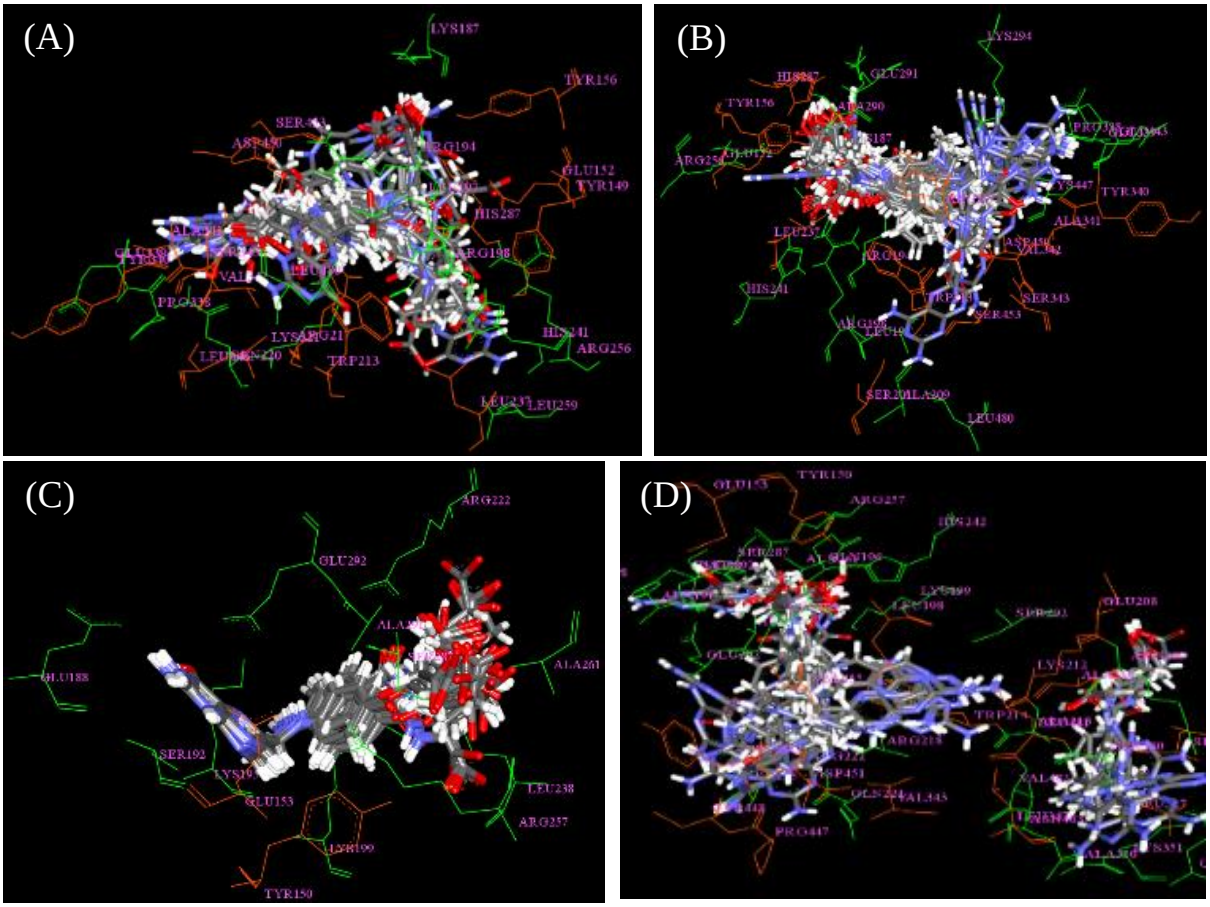


**Fig. S8.** Top 20 poses at the active site (ligand binding site) of protein according to the Total-score of Surflex-Docking experiment. (A) BSA-FA, (B) BSA-MTX, (C) HSA-FA, and (D) HSA-MTX docking study.

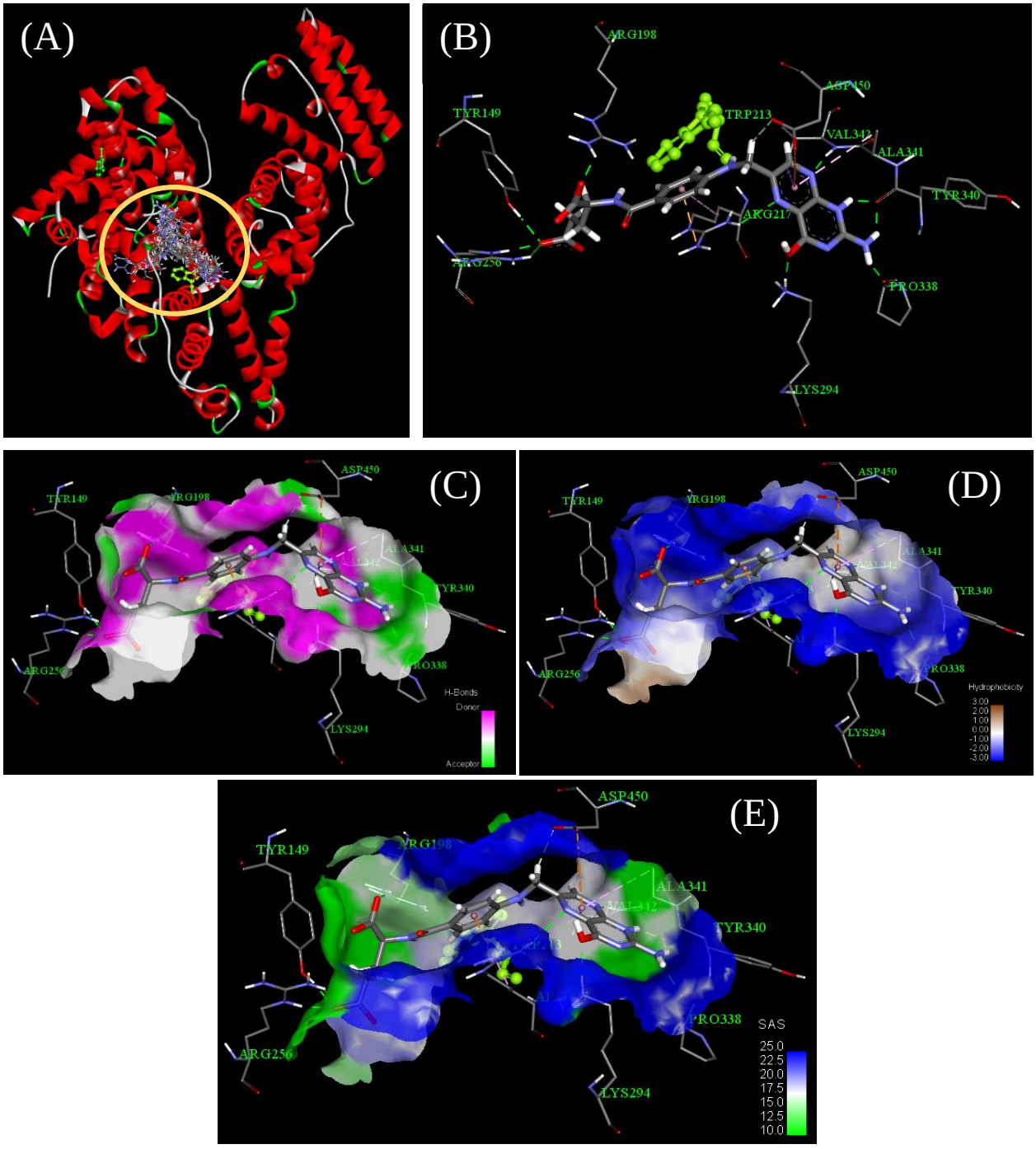


**Fig. S9.** Surflex-Docking results for BSA and FA. (A) Top 20 poses of FA in BSA; FA_0 at the active site of BSA showing (B) nonbonding Interaction, (C) hydrogen bond donor/acceptor surface, (D) hydrophobicity surface, (E) solvent accessibility surface.

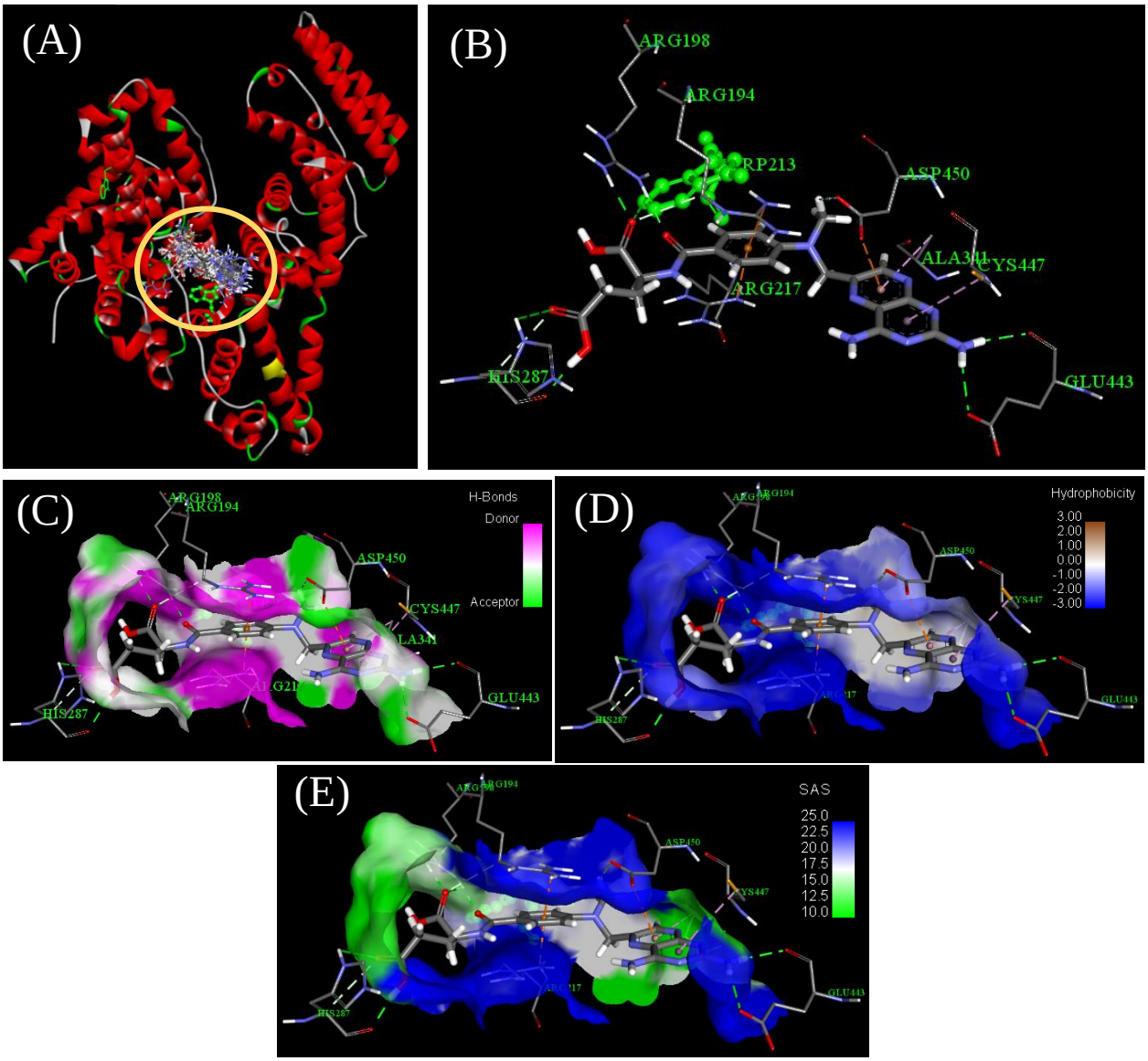


**Fig. S10.** Surflex-docking results for BSA and MTX. (A) Top 20 poses of MTX in BSA; MTX_0 at the active site of BSA showing (B) nonbonding interaction, (C) hydrogen bond donor/acceptor surface, (D) hydrophobicity surface, (E) solvent accessibility surface.

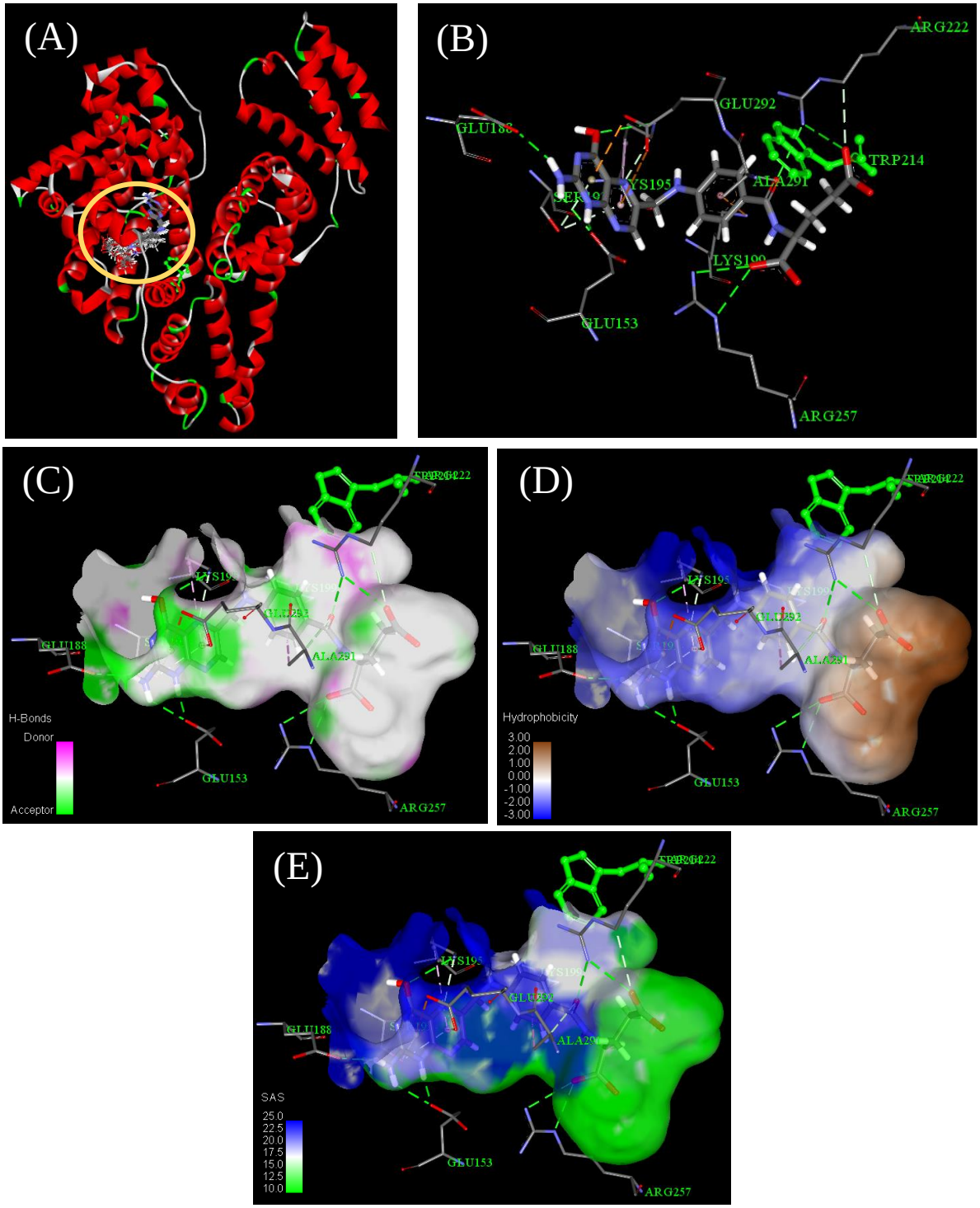


**Fig. S11.** Surflex-docking results for HSA and FA. (A) Top 20 poses of FA in HSA; FA_0 at the active site of HSA showing (B) nonbonding interaction, (C) hydrogen bond donor/acceptor surface, (D) hydrophobicity surface, (E) solvent accessibility surface.

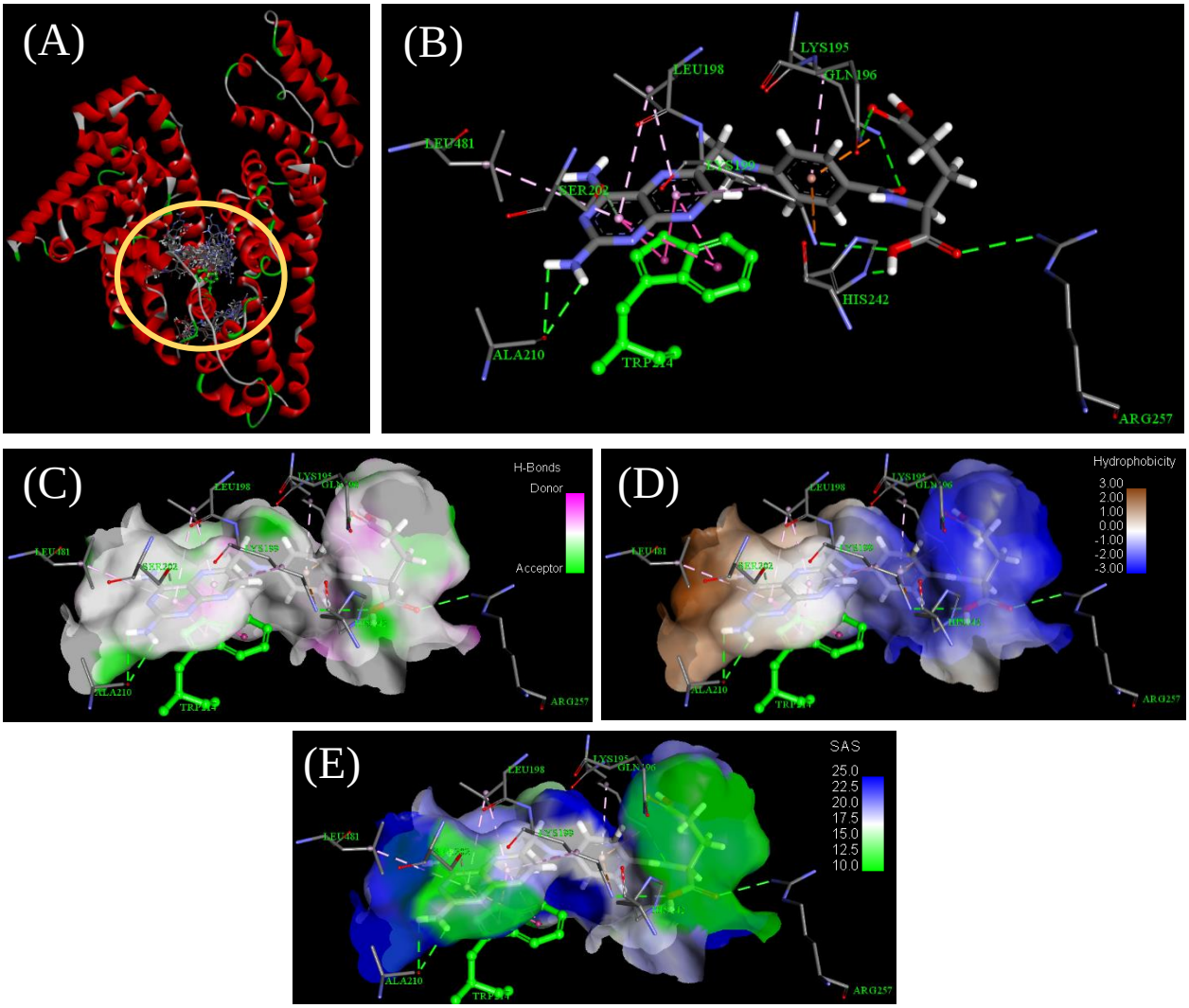


**Fig. S12.** Surflex-docking results for HSA and MTX. (A) Top 20 poses of MTX in HSA; MTX_0 at the active site of HSA showing (B) nonbonding interaction, (C) hydrogen bond donor/acceptor surface, (D) hydrophobicity surface, (E) solvent accessibility surface.

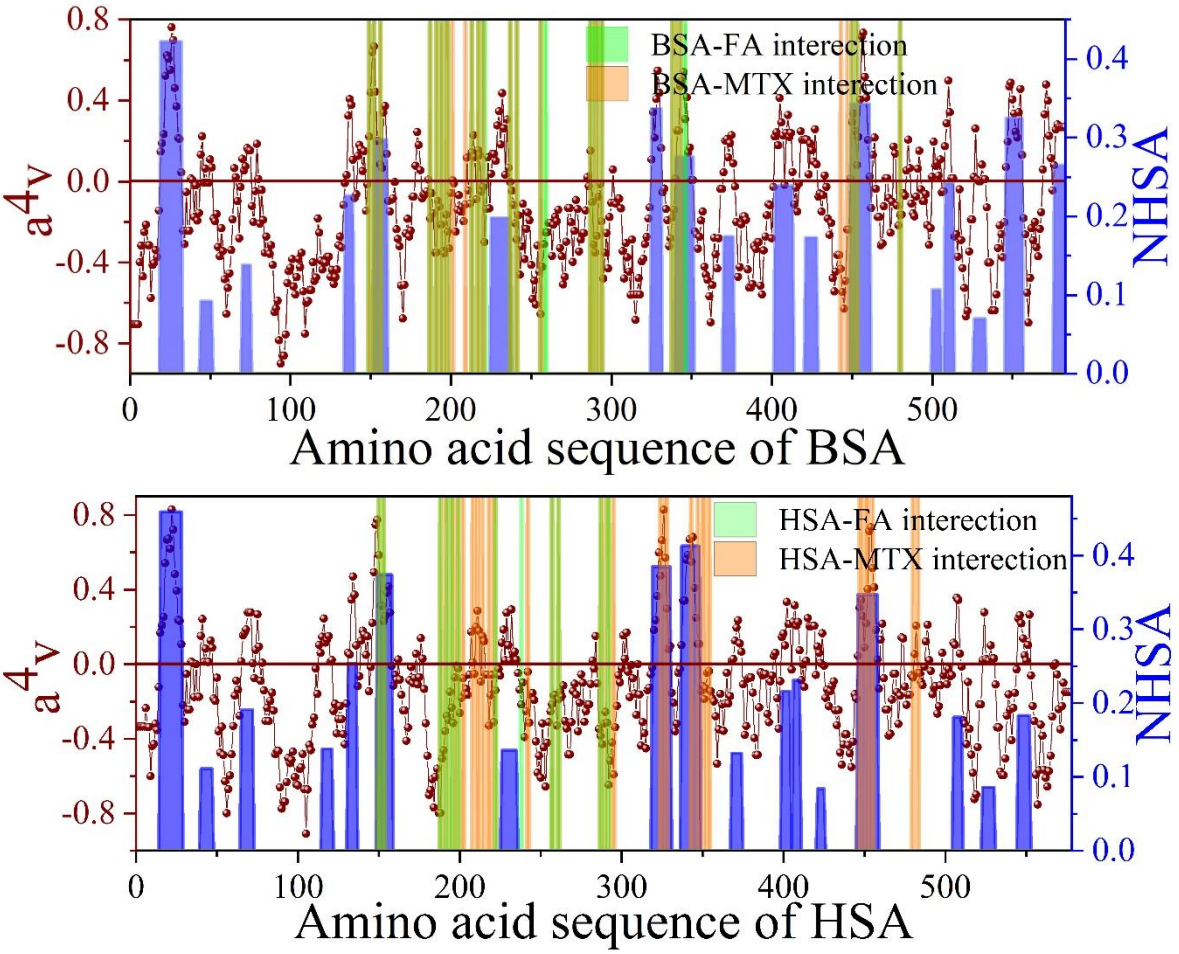


**Fig. S13.** Sequence analysis of aggregation-propensity of BSA and HSA by using AGGRESCAN tool. $a^4v$ and NHSA expressed window average of amino-acid aggregation-propensity and normalized hot-spot area per residue, respectively. Interacting residues with drugs from molecular docking studies have been shown as bar diagram.

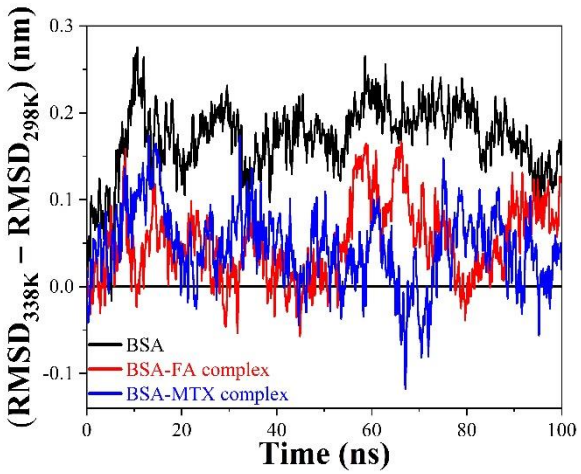


**Fig. S14.** Difference of RMSD values between 338K and 298K for BSA, BSA-FA and BSA-MTX complexes, as obtained from MD simulation.

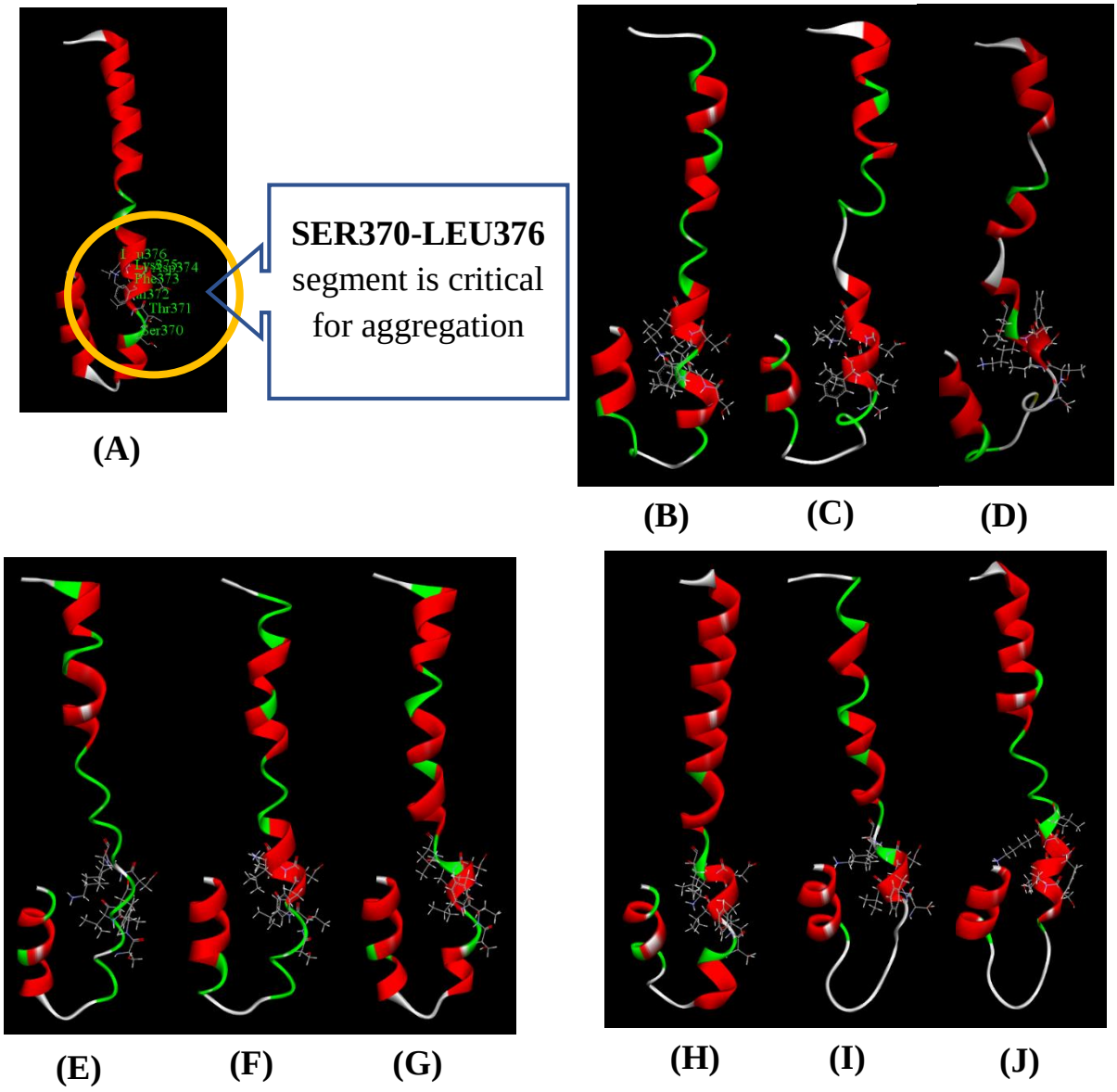


**Fig. S15.** (A) Crystal structure of BSA segment (LYS350 to TYR400). Segment (LYS350 to TYR400) of native BSA equilibrated at 338K for 10ns (B), 40ns (C), 100ns (D). Segment (LYS350 to TYR400) of BSA-FA complex equilibrated at 338K for 10ns (E), 40ns (F), 100ns (G). Segment (LYS350 to TYR400) of BSA-MTX complex equilibrated at 338K after 10ns (H), 40ns (I), 100ns (J).

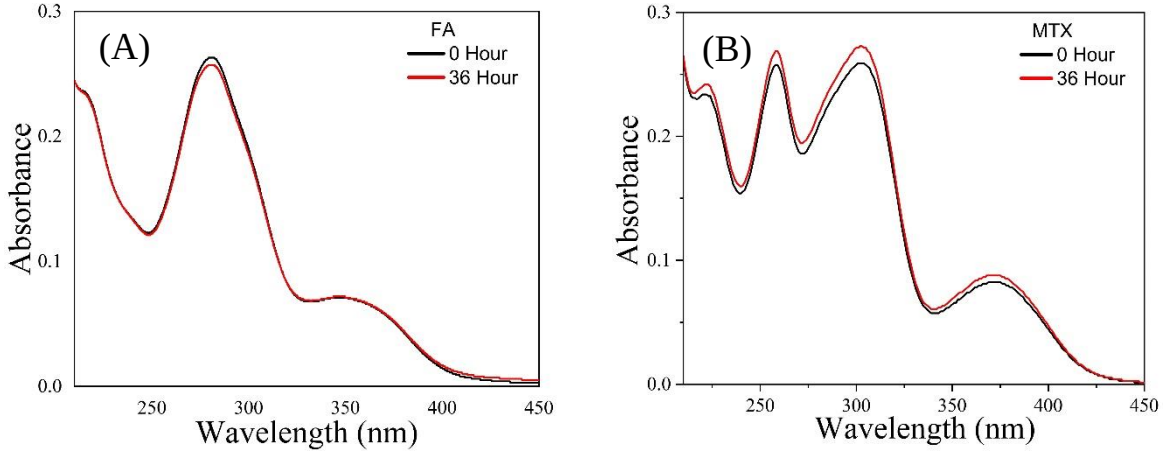


**Fig. S16.** Absorption spectra of FA (A) and MTX (B) before and after incubation for 36 hours at 65 $^0$C. The pH of the medium was maintained at 7.4 using phosphate buffer. During incubation at 65 $^0$C, the concentration of FA and MTX were kept 1.0 mM and 0.1 mM, respectively.

**Table S1.** Kinetic parameters of BSA fibrillation.

| | $F_\infty$ ($10^5$) | $\Delta F$ ($10^5$) | $k$ ($h^{-1}$) | $n$ |
|---|---|---|---|---|
| **BSA** | 5.8 | 5.8 | 0.1 | 0.8 |
| **BSA + 0.1 mM MTX** | 0.46 | 0.46 | 0.06 | 1.1 |
| **BSA + 1 mM FA** | 4.6 | 4.6 | 0.03 | 0.6 |

**Table S2.** Estimated Secondary Structure components of BSA in different systems from fitting of Circular Dichroism (CD) spectral data with DichroWeb® software.

| | Time (h) | α-helix (%) | β-sheet (%) | Turns (%) | Unordered (%) |
|---|---|---|---|---|---|
| 10 μM BSA | 0 | 54 | 13 | 11 | 22 |
| | 36 | 38 | 17 | 18 | 28 |
| 10 μM BSA + 0.1mM MTX | 0 | 56 | 13 | 10 | 21 |
| | 36 | 57 | 8 | 13 | 22 |

**Table S3.** SYBYL docking results.

| Surflex-Dock scores of FA at the active site of BSA | | | | | | | |
|---|---|---|---|---|---|---|---|
| Serial no. | Name | Total Score | Crash | Polar | PMF Score | G Score | Chem Score |
| 1 | FA_0 | 9.0 | -2.0 | 7.8 | -111 | -226 | -27 |
| 2 | FA_1 | 8.8 | -1.9 | 7.1 | -92 | -239 | -27 |
| 3 | FA_2 | 8.6 | -2.4 | 7.2 | -99 | -243 | -28 |
| 4 | FA_3 | 8.1 | -2.6 | 8.7 | -98 | -216 | -32 |
| 5 | FA_4 | 7.9 | -2.7 | 8.1 | -99 | -248 | -23 |
| 6 | FA_5 | 7.2 | -2.3 | 6.6 | -88 | -313 | -20 |
| 7 | FA_6 | 7.1 | -1.8 | 7.5 | -102 | -236 | -18 |
| 8 | FA_7 | 7.1 | -1.7 | 6.6 | -80 | -252 | -16 |
| 9 | FA_8 | 7.1 | -1.1 | 4.6 | -88 | -212 | -20 |
| 10 | FA_9 | 6.9 | -1.5 | 6.1 | -83 | -265 | -15 |
| 11 | FA_10 | 6.8 | -1.1 | 6.1 | -106 | -174 | -17 |
| 12 | FA_11 | 6.8 | -1.0 | 6.3 | -106 | -188 | -18 |
| 13 | FA_12 | 6.8 | -1.4 | 5.5 | -75 | -202 | -22 |
| 14 | FA_13 | 6.7 | -1.5 | 7.1 | -79 | -192 | -23 |
| 15 | FA_14 | 6.6 | -1.9 | 6.2 | -85 | -220 | -22 |
| 16 | FA_15 | 6.6 | -1.0 | 6.3 | -119 | -227 | -19 |
| 17 | FA_16 | 6.6 | -0.9 | 6.0 | -100 | -151 | -17 |
| 18 | FA_17 | 6.5 | -1.2 | 6.7 | -94 | -203 | -19 |
| 19 | FA_18 | 6.4 | -2.5 | 5.8 | -100 | -235 | -18 |
| 20 | FA_19 | 6.3 | -1.3 | 5.1 | -100 | -190 | -15 |
| 21 | FA_20 | 6.2 | -1.5 | 4.4 | -59 | -194 | -22 |
| **Surflex-Dock scores of MTX at the active site of BSA** | | | | | | | |
| 1 | MTX_0 | 9.3 | -0.9 | 5.6 | -75 | -210 | -21 |
| 2 | MTX_1 | 8.5 | -1.3 | 5.9 | -77 | -220 | -23 |

| | | | | | | | |
|---|---|---|---|---|---|---|---|
| 3 | MTX_2 | 8.2 | -1.2 | 5.4 | -85 | -197 | -22 |
| 4 | MTX_3 | 8.1 | -1.1 | 6.7 | -79 | -211 | -23 |
| 5 | MTX_4 | 8.0 | -1.3 | 6.0 | -81 | -208 | -22 |
| 6 | MTX_5 | 7.8 | -0.5 | 6.4 | -85 | -171 | -22 |
| 7 | MTX_6 | 7.6 | -2.4 | 6.9 | -80 | -208 | -18 |
| 8 | MTX_7 | 7.4 | -1.5 | 5.9 | -76 | -193 | -21 |
| 9 | MTX_8 | 7.4 | -1.0 | 3.1 | -104 | -219 | -18 |
| 10 | MTX_9 | 7.3 | -1.1 | 5.6 | -50 | -193 | -17 |
| 11 | MTX_10 | 7.3 | -1.4 | 5.0 | -102 | -222 | -16 |
| 12 | MTX_11 | 7.2 | -0.5 | 6.5 | -100 | -163 | -22 |
| 13 | MTX_12 | 7.2 | -1.4 | 6.1 | -77 | -189 | -20 |
| 14 | MTX_13 | 7.1 | -1.2 | 5.2 | -90 | -192 | -18 |
| 15 | MTX_14 | 7.1 | -1.1 | 4.8 | -82 | -201 | -17 |
| 16 | MTX_15 | 7.0 | -0.7 | 5.2 | -96 | -164 | -17 |
| 17 | MTX_16 | 7.0 | -1.3 | 4.6 | -78 | -199 | -17 |
| 18 | MTX_17 | 6.8 | -1.3 | 4.4 | -72 | -202 | -20 |
| 19 | MTX_18 | 6.7 | -0.9 | 4.7 | -71 | -178 | -16 |
| 20 | MTX_19 | 6.7 | -0.6 | 4.3 | -72 | -184 | -18 |
| 21 | MTX_20 | 6.6 | -0.6 | 4.1 | -93 | -158 | -11 |
| **Surflex-Dock scores of FA at the active site of HSA** | | | | | | | |
| 1 | FA_0 | 9.4 | -1.8 | 9.3 | -130 | -220 | -30 |
| 2 | FA_1 | 9.2 | -2.4 | 8.3 | -116 | -224 | -29 |
| 3 | FA_2 | 9.0 | -1.0 | 4.9 | -114 | -233 | -20 |
| 4 | FA_3 | 8.7 | -1.2 | 5.4 | -95 | -221 | -21 |
| 5 | FA_4 | 8.2 | -1.3 | 5.8 | -101 | -225 | -22 |
| 6 | FA_5 | 8.1 | -1.2 | 5.7 | -100 | -223 | -22 |
| 7 | FA_6 | 8.1 | -1.3 | 4.9 | -104 | -231 | -22 |

| | | | | | | | |
|---|---|---|---|---|---|---|---|
| 8 | FA_7 | 8.0 | -1.1 | 5.9 | -118 | -192 | -24 |
| 9 | FA_8 | 8.0 | -1.1 | 5.7 | -139 | -223 | -22 |
| 10 | FA_9 | 8.0 | -0.8 | 4.6 | -99 | -232 | -21 |
| 11 | FA_10 | 7.9 | -1.5 | 5.8 | -114 | -203 | -23 |
| 12 | FA_11 | 7.9 | -2.7 | 6.3 | -112 | -208 | -25 |
| 13 | FA_12 | 7.9 | -1.7 | 5.1 | -112 | -229 | -22 |
| 14 | FA_13 | 7.9 | -1.2 | 5.8 | -105 | -209 | -23 |
| 15 | FA_14 | 7.8 | -1.0 | 5.8 | -115 | -199 | -24 |
| 16 | FA_15 | 7.6 | -2.0 | 6.5 | -113 | -219 | -24 |
| 17 | FA_16 | 7.5 | -1.1 | 5.8 | -136 | -194 | -24 |
| 18 | FA_17 | 7.4 | -1.6 | 5.8 | -106 | -205 | -23 |
| 19 | FA_18 | 7.4 | -2.1 | 5.1 | -105 | -216 | -23 |
| 20 | FA_19 | 7.4 | -1.6 | 5.7 | -94 | -220 | -22 |
| 21 | FA_20 | 7.4 | -1.3 | 5.7 | -112 | -210 | -23 |
| **Surflex-Dock scores of MTX at the active site of HSA** | | | | | | | |
| 1 | MTX_0 | 8.0 | -1.7 | 5.3 | -136 | -211 | -32 |
| 2 | MTX_1 | 7.5 | -0.4 | 4.9 | -49 | -245 | -22 |
| 3 | MTX_2 | 7.4 | -1.5 | 5.5 | -118 | -203 | -30 |
| 4 | MTX_3 | 6.9 | -1.1 | 6.2 | -93 | -174 | -31 |
| 5 | MTX_4 | 6.7 | -1.4 | 4.6 | -136 | -196 | -28 |
| 6 | MTX_5 | 6.4 | -1.7 | 3.9 | -146 | -207 | -26 |
| 7 | MTX_6 | 6.4 | -1.2 | 3.5 | -141 | -213 | -25 |
| 8 | MTX_7 | 6.2 | -1.7 | 4.6 | -117 | -182 | -29 |
| 9 | MTX_8 | 6.2 | -1.2 | 4.3 | -67 | -208 | -27 |
| 10 | MTX_9 | 6.1 | -1.3 | 3.6 | -144 | -205 | -26 |
| 11 | MTX_10 | 6.0 | -0.7 | 5.5 | -94 | -144 | -27 |
| 12 | MTX_11 | 5.8 | -1.3 | 3.5 | -162 | -219 | -26 |

| | | | | | | | |
|---|---|---|---|---|---|---|---|
| 13 | MTX_12 | 5.8 | -1.5 | 3.7 | -133 | -196 | -19 |
| 14 | MTX_13 | 5.8 | -1.1 | 4.3 | -158 | -157 | -21 |
| 15 | MTX_14 | 5.7 | -0.8 | 5.0 | -90 | -154 | -24 |
| 16 | MTX_15 | 5.7 | -0.6 | 4.5 | -28 | -185 | -22 |
| 17 | MTX_16 | 5.6 | -1.4 | 4.2 | -102 | -173 | -27 |
| 18 | MTX_17 | 5.5 | -0.7 | 4.6 | -26 | -202 | -23 |
| 19 | MTX_18 | 5.5 | -1.2 | 3.8 | -38 | -225 | -22 |
| 20 | MTX_19 | 5.4 | -0.5 | 5.4 | -75 | -193 | -23 |
| 21 | MTX_20 | 4.9 | -1.0 | 4.6 | -23 | -198 | -22 |

**Table S4.** Nonbonding interaction of BSA and HSA with FA and MTX, respectively. Blue-marked residues have critical aggregation-propensity value.

| **Nonbonding Interaction of BSA residue with FA** | |
|---|---|
| **Name** | **Type of interaction** |
| TYR149 | Hydrogen Bond |
| GLU152 | Hydrogen Bond, Electrostatic |
| TYR156 | Hydrogen Bond |
| LYS187 | Hydrogen Bond, Hydrophobic |
| SER191 | Hydrogen Bond |
| ARG194 | Hydrogen Bond, Electrostatic, Hydrophobic |
| LEU197 | Hydrophobic |
| ARG198 | Hydrogen Bond, Electrostatic |
| TRP213 | Hydrogen Bond |
| ARG217 | Hydrogen Bond, Electrostatic, Hydrophobic |
| GLN220 | Hydrogen Bond |
| LYS221 | Hydrogen Bond |
| LEU237 | Hydrophobic |
| HIS241 | Hydrogen Bond |
| ARG256 | Hydrogen Bond, Hydrophobic |
| LEU259 | Hydrophobic |
| HIS287 | Hydrophobic |
| ILE289 | Hydrophobic |
| ALA290 | Hydrophobic |
| GLU291 | Hydrogen Bond |
| LYS294 | Hydrogen Bond, Electrostatic |
| PRO338 | Hydrogen Bond |
| GLU339 | Hydrogen Bond |
| TYR340 | Hydrogen Bond |
| ALA341 | Hydrophobic |
| VAL342 | Hydrogen Bond, Hydrophobic |
| SER343 | Hydrogen Bond |
| LEU346 | Hydrophobic |
| ASP450 | Hydrogen Bond, Electrostatic |

| | |
|---|---|
| SER453 | Hydrogen Bond |
| LEU480 | Hydrophobic |
| **Nonbonding Interaction of BSA residue with MTX** | |
| GLU152 | Electrostatic |
| TYR156 | Hydrogen Bond |
| LYS187 | Hydrogen Bond, Hydrophobic |
| SER191 | Hydrogen Bond |
| ARG194 | Hydrogen Bond, Electrostatic, Hydrophobic |
| LEU197 | Hydrophobic |
| ARG198 | Hydrogen Bond |
| SER201 | Hydrogen Bond |
| ALA209 | Hydrogen Bond |
| TRP213 | Hydrogen Bond |
| ARG217 | Hydrogen Bond, Electrostatic |
| LEU237 | Hydrophobic |
| HIS241 | Electrostatic |
| ARG256 | Hydrogen Bond |
| HIS287 | Hydrogen Bond |
| ALA290 | Hydrogen Bond, Hydrophobic |
| GLU291 | Hydrogen Bond |
| LYS294 | Hydrogen Bond |
| PRO338 | Hydrogen Bond |
| GLU339 | Hydrogen Bond |
| TYR340 | Hydrogen Bond, Hydrophobic |
| ALA341 | Hydrophobic |
| VAL342 | Hydrogen Bond, Hydrophobic |
| SER343 | Hydrogen Bond |
| GLU443 | Hydrogen Bond |
| CYS447 | Hydrophobic |
| ASP450 | Hydrogen Bond, Electrostatic |
| SER453 | Hydrogen Bond |
| LEU480 | Hydrophobic |

| Nonbonding Interaction of HSA residue with FA | |
|---|---|
| TYR150 | Hydrogen Bond |
| GLU153 | Hydrogen Bond |
| GLU188 | Hydrogen Bond |
| SER192 | Hydrogen Bond |
| LYS195 | Hydrogen Bond, Hydrophobic |
| LYS199 | Hydrogen Bond, Electrostatic |
| ARG222 | Hydrogen Bond |
| LEU238 | Hydrogen Bond |
| ARG257 | Hydrogen Bond, Electrostatic |
| ALA261 | Hydrogen Bond |
| SER287 | Hydrogen Bond |
| ALA291 | Hydrogen Bond, Hydrophobic |
| GLU292 | Electrostatic |
| **Nonbonding Interaction of HSA residue with MTX** | |
| TYR150 | Hydrogen Bond |
| GLU153 | Hydrogen Bond |
| GLU188 | Hydrogen Bond |
| ALA191 | Hydrogen Bond |
| SER192 | Hydrogen Bond |
| LYS195 | Hydrogen Bond, Electrostatic, Hydrophobic |
| GLN196 | Hydrogen Bond |
| LEU198 | Hydrophobic |
| LYS199 | Hydrogen Bond, Electrostatic, Hydrophobic |
| SER202 | Hydrogen Bond |
| GLU208 | Hydrogen Bond |
| ARG209 | Hydrogen Bond, Electrostatic, Hydrophobic |
| ALA210 | Hydrogen Bond |
| LYS212 | Hydrogen Bond |
| ALA213 | Hydrophobic |
| TRP214 | Hydrogen Bond, Hydrophobic |
| ARG218 | Hydrogen Bond, Electrostatic |

| | |
|---|---|
| GLN221 | Hydrogen Bond |
| ARG222 | Hydrogen Bond, Electrostatic |
| HIS242 | Hydrogen Bond |
| ARG257 | Hydrogen Bond |
| ALA261 | Hydrogen Bond |
| SER287 | Hydrogen Bond |
| HIS288 | Hydrogen Bond |
| ALA291 | Hydrogen Bond, Hydrophobic |
| GLU292 | Hydrogen Bond, Electrostatic |
| ASN295 | Hydrogen Bond |
| ASP324 | Hydrogen Bond |
| LEU327 | Hydrogen Bond |
| VAL343 | Hydrophobic |
| LEU347 | Hydrogen Bond, Hydrophobic |
| ALA350 | Hydrophobic |
| LYS351 | Electrostatic, Hydrophobic |
| GLU354 | Hydrogen Bond, Electrostatic |
| PRO447 | Hydrogen Bond, Hydrophobic |
| CYS448 | Hydrogen Bond, Hydrophobic |
| VAL455 | Hydrophobic |
| ASP451 | Hydrogen Bond, Electrostatic |
| TYR452 | Hydrophobic |
| SER480 | Hydrogen Bond |
| LEU481 | Hydrophobic |
| VAL482 | Hydrophobic |
| ASN483 | Hydrogen Bond |

**Table S5.** Important residues of proteins having tendency to induce amyloid aggregation as per aggregation propensity calculations

| BSA | HSA |
|---|---|
| TYR149, GLU152, TYR156, SER201, TRP213, ARG217, LEU237, HIS287, TYR340, ALA341, VAL342, SER343, ASP450, SER453 | TYR150, GLU153, LEU198, GLU208, ALA210, LYS212, TRP214, ASP324, LEU327, VAL343, LEU347, PRO447, CYS448, ASP451, TYR452, VAL455, LEU481 |

## REFERENCES


1. L. Whitmore and B. A. Wallace, *Nucleic Acids Res.*, 2004, **32**, W668-W673.
2. L. Whitmore and B. A. Wallace, *Biopolymers*, 2008, **89**, 392-400.
3. M. Dasgupta and N. Kishore, *PLoS One*, 2017, **12**, e0172208.
4. S. Saha and S. Deep, *J. Phys. Chem. B*, 2014, **118**, 9155-9166.
5. O. Conchillo-Solé, N. S. de Groot, F. X. Avilés, J. Vendrell, X. Daura and S. Ventura, *BMC Bioinf.*, 2007, **8**, 65.
6. A. Bujacz, *Acta Crystallogr. D Biol. Crystallogr.*, 2012, **68**, 1278-1289.
7. S. Sugio, A. Kashima, S. Mochizuki, M. Noda and K. Kobayashi, *Protein Eng.*, 1999, **12**, 439-446.
8. H. J. C. Berendsen, D. Van der Spoel and R. Van Drunen, *Comp. Phys. Comm.*, 1995, **91**, 43-56.
9. M. J. Abraham, T. Murtola, R. Schulz, S. Páll, J. C. Smith, B. Hess and E. Lindahl, *SoftwareX*, 2015, **1**, 19-25.
10. L. S. Dodda, I. Cabeza de Vaca, J. Tirado-Rives and W. L. Jorgensen, *Nucleic Acids Res.*, 2017, **45**, W331-W336.
11. W. L. Jorgensen, D. S. Maxwell and J. Tirado-Rives, *J. Am. Chem. Soc.*, 1996, **118**, 11225-11236.
12. P. Khatua, S. Mondal and S. Bandyopadhyay, *J. Chem. Inf. Model.*, 2019, **59**, 2879-2893.
13. S. Millan, L. Satish, K. Bera and H. Sahoo, *New J. Chem.*, 2019, **43**, 3956-3968.


--